Study of the neutrino electromagnetic properties with prototype of BOREXINO detector

H.O. Back, M. Balata, A. de Bari, T. Beau, A. de Bellefon, G. Bellini, J. Benziger, S. Bonetti, C. Buck, B. Caccianiga, et al.

ОБЪЕДИНЕННЫЙ
ИНСТИТУТ
ЯДЕРНЫХ
ИССЛЕДОВАНИЙ

Дубна

E1-2002-29

STUDY OF THE NEUTRINO ELECTROMAGNETIC PROPERTIES WITH PROTOTYPE OF BOREXINO DETECTOR

Submitted to «Physics Letters B»

2002

H. O. Back[1], M. Balata[2], A. de Bari[3], T. Beau[4], A. de Bellefon[4], G. Bellini[5], J. Benziger[6], S. Bonetti[5], C. Buck[7], B. Caccianiga[5], L. Cadonati[6], F. Calaprice[6], G. Cecchet[3], M. Chen[8], A. Di Credico[2], O. Dadoun[4], D. D'Angelo[9], A. Derbin[10], M. Deutsch[11], F. Elisei[12], A. Etenko[13], F. von Feilitzsch[14], R. Fernholz[6], R. Ford[6], D. Franco[5], B. Freudiger[7], C. Galbiati[6], F. Gatti[9], S. Gazzana[2], M. G. Giammarchi[5], D. Giugni[5], M. Goeger-Neff[14], A. Golubchikov, A. Goretti[2], C. Grieb[14], C. Hagner[1], T. Hagner[14], W. Hampel[7], B. Harding[6], F. X. Hartmann[7], G. Heusser[7], A. Ianni[5,6], A. M. Ianni[6], H. de Kerret[4], J. Kiko[7], T. Kirsten[7], G. Korga[5,15], G. Korschinek[14], Y. Kozlov[13], D. Kryn[4], M. Laubenstein[2], C. Lendvai[14], P. Lombardi[5], I. Machulin[13], S. Malvezzi[1], J. Maneira[1], I. Manno[15], G. Manuzio[9], F. Masetti[12], A. Martemianov[2,13], U. Mazzucato[12], K. McCarty[6], E. Meroni[5], L. Miramonti[5], M. E. Monzani[2,5], P. Musico[9], H. Neder[7], L. Niedermeier[14], L. Oberauer*, M. Obolensky[4], F. Ortica[12], M. Pallavicini[9], L. Papp[5,15], L. Perasso[5], A. Pocar[6], R. S. Raghavan[16], G. Ranucci[5], W. Rau[2,7], A. Razeto[9], E. Resconi[9], A. Sabelnikov[5,13], C. Salvo[9], R. Scardaoni[5], S. Schoenert[7], H. Seidel[14], H. Simgen[7], T. Shutt[6], M. Skorokhvatov[13], O. Smirnov, A. Sonnenschein[6], A. Sotnikov, S. Sukhotin[13], V. Tarasenkov[13], R. Tartaglia[2], G. Testera[9], D. Vignaud[4], S. Vitale[9], R. B. Vogelaar[1], V. Vyrodov[13], M. Wojcik[17], O. Zaimidoroga, G. Zuzel[17]

[1]Virginia Polytechnique Institute and State University, Blacksburg, VA 24061-0435, Virginia, USA
[2]LNGS, Assergi (AQ), Italy
[3]Dipartimento di Fisica Nucleare e Teorica Universita' di Pavia, Pavia, Italy
[4]Laboratoire de Physique Corpusculaire et Cosmologie, 75231 Paris Cedex 05, France
[5]Dipartimento di Fisica Universita' di Milano, Milano, Italy
[6]Department of Physics, Princeton University, Princeton NJ 08544-0708, USA
[7]Max-Planck-Institut fuer Kernphysik, Heidelberg, Germany
[8]Department of Physics, Queen's University, Stirling Hall, Kingston, Ontario K7L 3N6, Canada
[9]Dipartimento di Fisica Universita' and INFN, Genova, Italy
[10]St. Petersburg Nuclear Physics Institute, Gatchina, Russia
[11]Department of Physics, Massachusetts Institute of Technology, Cambridge, MA 02139, USA
[12]Dipartimento di Chimica, Universita' di Perugia, Perugia, Italy
[13]RRC Kurchatov Institute, Moscow, Russia
[14]Technische Universitaet Muenchen, Garching, Germany
[15]KFKI-RMKI, Budapest, Hungary
[16]Bell Laboratories, Lucent Technologies, Murray Hill, NJ 07974-2070, USA
[17]Institute of Physics, Jagellonian University, Krakow, Poland
*Project manager

1 Introduction

A Lorentz-covariant total electromagnetic current of the fermions can be presented in the following form [1]:

$$J_\alpha(q) = F(q^2)\gamma_\alpha + G(q^2)(q^2\gamma_\alpha - 2i(q_\alpha))\gamma_5 + M(q^2)\sigma_{\alpha,\beta}q_\beta + iE(q^2)\sigma_{\alpha,\beta}q_\beta\gamma_5 \quad (1)$$

where q is four momenta transferred and the functions $F(q^2)$, $G(q^2)$, $M(q^2)$ and $E(q^2)$ are usually referred to as an electromagnetic, anapole, magnetic and electric dipole form factors, respectively. Assuming charge conservation in a decay $n \to p + e^- + \bar{\nu}_e$, experimental measurements of the charge of $(p + e^-)$ [12] and neutron [3] lead to upper limit $|e_{\overline{\nu_e}}| \leq 10^{-21}e$. From the astrophysical data including the solar data and the SN1987A the limits on the neutrino charge are less stringent $e_\nu \leq 10^{-13} \div 10^{-17}e$ [4],[5].

The charge radius of neutrino $< r^2 > \simeq 6\frac{\delta F(q^2)}{\delta q^2}\mid_{q^2=0}$ (as well as anapole moment for the Majorana neutrino) is induced by the radiative corrections in Standard Model (SM) and has a value $\frac{G_F}{2\sqrt{2}\pi^2} ln\frac{M_W^2}{m_e^2} \sim 3.2 \times 10^{-33}\, cm^2$ for the electron neutrino [6],[7]. The modern experiments on accelerators studing the $(\nu_\mu, e)-$scattering have the sensitivity about one order of magnitude lower than needed to see effect of these radiative corrections [8, 9, 10].

The neutrino magnetic moment $\mu_\nu = M(0)$ in SM is proportional to the neutrino mass, which is causing the neutrino helicity flip responsible for the generation of the magnetic moment. The value of the μ_ν is

$$\mu_\nu = \frac{3m_e G_F}{4\pi\sqrt{2}} m_\nu \mu_B \approx 3.210^{-19}(\frac{m_\nu}{1eV})\mu_B \, . \quad (2)$$

The modern limit on the neutrino mass is 2.5 eV[11], hence the neutrino magnetic moment calculated in the frames of the Standard Model is about $10^{-18}\mu_B$, where $\mu_B = \frac{eh}{4\pi m_e}$ is electron Bohr magneton. A nonzero neutrino electric dipole moment $d_\nu = E(0)$ requires CP violation and up to now such moment has not been observed for any other particle. Both dipole moments (μ_ν, d_ν) are forbidden for Majorana neutrinos in the case of CPT-invariance.

In the case when neutrinos are mixed, the matrix of the electromagnetic moments μ_{ik} (d_{ik}) will replace the form factors $M(E)$ in (1). The indexes $i, k = 1.2.3$ mean the mass eigenstates of neutrino. The matrix describes the transitions between mass and flavour eigenstates. The diagonal elements of the matrix vanishes for the Majorana neutrino. The non-diagonal elements of the matrix (transition moments) lead to the scattering with the neutrino of another flavour in the final state or to the radiative neutrino decay $\nu_H \to \nu_L + \gamma$. The life time of neutrino expressed in the terms of the transition magnetic moment is [12]:

$$\tau[s] \approx 0.19(\frac{\mu_B}{\mu_{HL}^{eff}})^2(\frac{m_{\nu_H}^2}{m_{\nu_H}^2 - m_{\nu_L}^2})(\frac{1eV}{m_{\nu_H}})^3, \quad (3)$$

where $(\mu_{HL}^{eff})^2 = (\mu_{HL})^2 + (d_{HL})^2$ is the sum of magnetic and electric transition moments.

In the present paper the results of the search for the neutrino magnetic moment and neutrino radiative decay with the prototype of the Borexino detector are presented.

For a long time, the negative result of experiments on the search for neutrino-electron interactions were interpreted as a limitation on the possible magnetic moment of neutrino [13],[14]. From the middle of 1980's the neutrino magnetic moment hypothesis is widely discussed in the context of the astrophysical motivations. The neutrino flux measured by Cl-Ar detector seemed to show a significant time variation in correlation with solar magnetic activity as reported in [15]-[17]. In publications [18]-[20] was shown that this correlation can be caused by the interaction of the neutrino magnetic moment with magnetic field in the convective zone of Sun. This interaction leads to a reversal of neutrino helicity converting left-handed neutrino into the right-handed one, which is not participating in the reactions with charged currents. The value of the magnetic moment required for the observation of such variations with operating solar neutrino detectors lies in the range of $(10^{-10} - 10^{-11})\mu_B$. At present Homestake data are still analyzed for the possible time variations [21],[22].

Magnetically induced spin-flavour oscillations also provide a suitable solution of the solar neutrino problem [23]-[26].

The value 10^{-10} μ_B is eight order of magnitude higher than the value predicted by Standard theory, but does not contradict the restriction obtained in laboratory experiments. Elastic scattering of a neutrino by an electron turns out to be the most sensitive to the neutrino magnetic moment reaction. The measured values of the cross-section of this process set the restriction $\mu_{\overline{\nu_e}} \leq 1.8 \times 10^{-10}$ μ_B on possible magnetic moment for electron antineutrinos [27], $\mu_{\nu_e} \leq 1.1 \times 10^{-9}$ μ_B for electron neutrino [28], $\mu_{\nu_\mu} \leq 6.8 \times 10^{-10}$ μ_B for muon neutrinos [28] and $\mu_{\nu_\tau} \leq 3.9 \times 10^{-7}$ μ_B for tau-neutrinos [29]. The astrophysical limitations, based mainly on the fact that scattering of neutrinos with a large magnetic moment by charged particles leads to the intensive production of right neutrinos that don't participate in weak interaction, and, hence change the dynamics of stars, lay in the region $10^{-10} - 10^{-11}$ μ_B [30]. The observation of neutrinos formed as a result of a burst of supernova SN1987A has led to stronger restrictions up to 10^{-12} μ_B ([4],[30] and references therein). As concerning the solar neutrino, upper bound on ^8B-neutrino magnetic moment was obtained in [31], $\mu_\nu \leq 2.2 - 2.3 \times 10^{-10}$ μ_B using the data from SuperKamiokande, Kamiokande and Homestake. More recent analysis of the Superkamiokande ^8B-data sets the limit on the neutrino magnetic moment $\mu_\nu \leq 1.5 \times 10^{-10}$ μ_B (90% c.l.)[32]. In this work it was shown that the neutrino magnetic moment μ_ν in the certain oscillation scenarious can differ from the measured in the reactor experiments. One can see that obtained experimental bounds are far from value predicted by the standard model where the small value of magnetic moment is caused by its proportionality to the neutrino mass. However, in models with right

bosons or with an extended sector of scalar particles, the magnetic moment can be proportional to the mass of intermediate lepton and can attain the values indicated earlier [33],[34].

2 Experimental set-up (Counting Test Facility) and results of measurements

Borexino, a real-time detector for low energy neutrino spectroscopy, is near completion in the underground laboratory at Gran Sasso (see recent [35] and references therein). The main goal of the detector is the direct measurement of the flux of ^7Be solar neutrinos of all flavours via neutrino-electron scattering in an ultra-pure liquid scintillator. Borexino will also address several other frontier questions in particle physics, astrophysics and geophysics.

The CTF was constructed and installed in Hall C of the Gran Sasso Laboratory. The main goal of the CTF was to test the key concept of Borexino, namely the possibility to purify a large mass of liquid scintillator at the level of contamination in U and Th of a few units 10^{-16} g/g. This goal was successfully achieved with the first prototype (CTF-I,[36]) operated in 1995-1997. The detector was reinstalled in 1999 (CTF-II,[37]) with the purpose of serving as a facility for the quality control of the pseudocumene to be delivered for the Borexino experiment. Although the CTF is a large-scale detector (4 tons of liquid scintillator), its size is nonetheless modest in comparison to Borexino (300 tons). The view of the CTF detector is presented in fig.1. A mass in the 4 ton range was set by the need to make the prevailing scintillator radioimpurities measurable via delayed coincidence tagged events[1], while a water shield thickness of approximately 4.5 m was needed in order to suppress the external radiation. The primary goal of the CTF was to develop a solution directly applicable to operational issues for Borexino; in the future there will be also the long-range goal of performing quality control during Borexino operations. Detailed reports on the CTF have been published [36],[35]-[40]. As a simplified scaled version of the Borexino detector, a volume of liquid scintillator is contained in a 2 m diameter transparent inner nylon vessel mounted at the center of an open structure that supports 100 phototubes (PMT) [41] which detect the scintillation signals. The whole system is placed within a cylindrical tank (11m in diameter and 10m height) that contains 1000 tons ultra-pure water, which provides a shielding against neutrons originating from the rock and against external γ-rays from PMT's and other construction materials. The scintillator used for the major part of tests in the CTF-I was a binary mixture consisting of pseudocumene[2] (PC) as a solvent and 1.5 g/l of PPO (2,5-diphenyloxazole) as a fluor. The CTF-II data analyzed in the present paper are acquired with an alternate liquid scintillator sol-

[1] Key components in the decay chains of U/Th and in the β-decay of ^{85}Kr are emitted as time-correlated coincidence pairs which can be tagged with high specificity.

[2] 1,2,4-trimethylbenzene C_9H_{12}

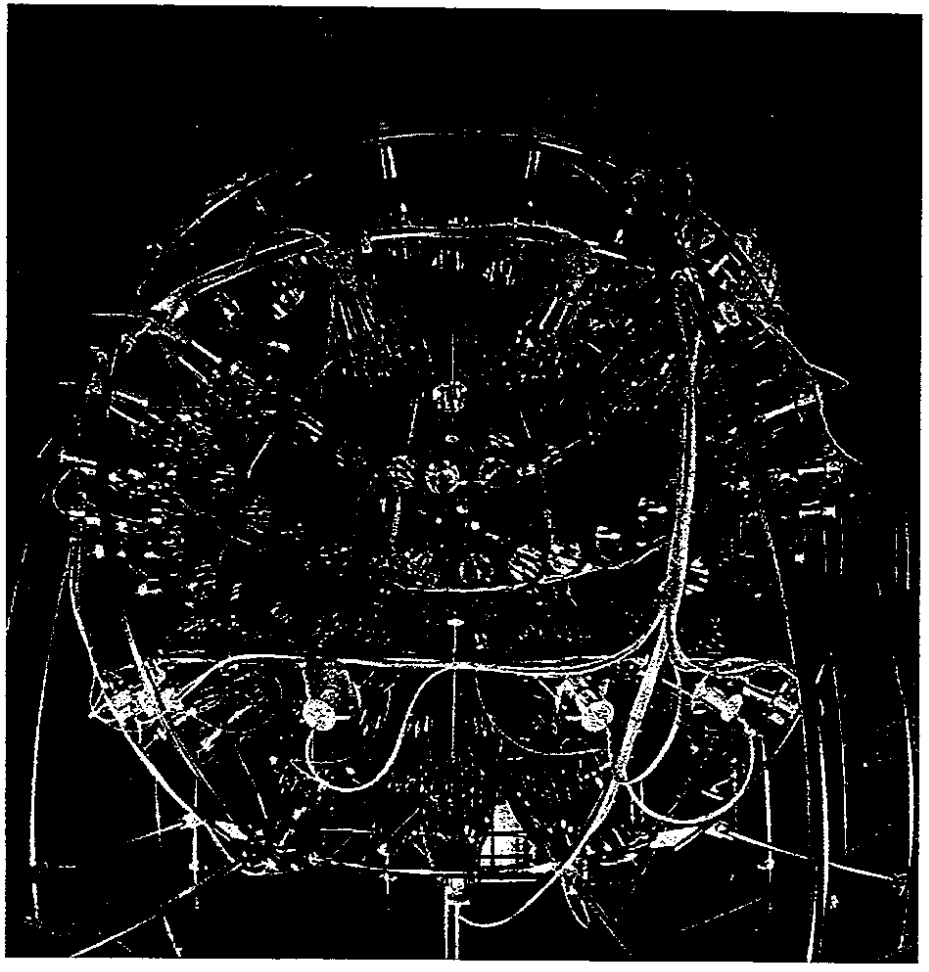

Figure 1: The view of the CTF detector

vent, phenylxylylethane (PXE, $C_{16}H_{18}$)[3]. The scintillator is carefully purified to ensure the ^{238}U and ^{232}Th in it are less than some units 10^{-16} g/g. The PMT's are 8 inch ETL 9351 tubes made of low radioactivity glass and characterized by high quantum efficiency (26% at 420 nm), limited transit time spread (1 ns) and good pulse height resolution for single photoelectron pulses (Peak/Valley = 2.5). The number of photoelectrons registered by one PMT for the 1 MeV energy deposit at the detector's center is about 3.5 for the PXE.

[3]with p-diphenylbenzene (para-terphenyl) as a primary wavelength shifter at a concentration of 3 g/l along with a secondary wavelength shifter 1,4-bis (2-methylstyrol) benzene (bis-MSB) at the 50 mg/l

3 Data analysis and results.

3.1 Response function of the CTFII detector

The energy of an event in the CTF detector is defined using the total collected charge from all PMTs. In the simple approach the energy is supposed to be linear in respect to the total collected charge. The dependence of the total collected charge on the event position is not taken into account in this approach. This will cause errors in the energy calculated for the point-like sources at the definite position inside the CTF. Nevertheless, for the events distributed uniformly over the CTF inner vessel the mean value of the registered charge has a linear dependence on the event energy. The coefficient linking the event energy and the total collected charge we will call light (or photoelectrons) yield. The light yield for the electrons can be considered linear with respect to its energy only for the high energies. At the lower energies the phenomenon of the "ionization quenching" violates the linear dependence of the light yield on energy [42]. The effect on the electrons and gammas light yield is discussed in [43]. We used for the calculation the parameterization of the light yield dependence on energy $f(E)$ with three fixed parameters in the following form:

$$f(E) \equiv 1 - \frac{Y(E)}{Y(\infty)} = 1 - C_1 exp(-\frac{E^{C_2}}{C_3}). \quad (4)$$

Because of the nonlinear dependence of the light yield on the energy released due to the ionization quenching effect, the CTF resolution should be expressed in the terms of the total registered charge, which is directly measured in the experiment.

The study with the radioactive sources placed at the different positions inside the CTF inner vessel showed that the CTF response can be approximated by a Gaussian with the sigma defined by the following formula:

$$\sigma_Q = \sqrt{(1 + \overline{v_1})Q + v_p Q^2}, \quad (5)$$

where

$Q = A \cdot E \cdot f(k_B, E) \cdot v_f$ is mean total registered charge for the events of the energy E distributed over the detector's volume;

$\overline{v_1} = \frac{1}{N_{PM}} \sum_{i=1}^{N_{PM}} s_i v_{1_i} = 0.34$ is the relative variance of the PMT single photoelectron charge spectrum (v_{1_i}) averaged over all CTF PMTs (N_{PM}), taking into account the i-th PMT relative sensitivity s_i;

$A = 350$ is scintillator specific light yield measured in photoelectrons per MeV ($A \equiv \frac{Y(\infty)}{E}$, A=350 p.e./MeV in CTF-II for the event at the detector's center);

$f(E)$ is the function taking into account ionization quenching, the function is defined by (4);

$v_p = 0.0023$ is the parameter which takes into account the variance of the signal for the source uniformly distributed over the detector's volume. The parameter gives additional signal variance for the source distributed over the detector's volume in comparison to the point-like source at the detector's center. The last case will naturally yield $v_p = 0$.

$v_f = 1.005$ is volume factor, coming from the averaging of the signals over the CTF volume.

All the parameters in (5) were defined with satisfactory precision from the CTF-II data (see [44],[45] for the details). The radial dependence of the detector response was defined from the experimental data as well.

For the estimations of the energy resolution one can use approximation $\frac{\sigma_E}{E} \approx \frac{\sigma_Q}{Q}$.

3.2 Backgrounds and data selection

In our analysis we used the data obtained with an upgrade of the CTF detector, CTF-II. The detector, loaded with the PXE, is equipped with an additional nylon bag (radon shroud) intended to reduce the radon diffusion from the construction materials into the scintillator.

The data obtained during 32.1 days of the CTF-II run were used. The major part of the CTF background in the energy region up to 200 keV is induced by β-activity of ^{14}C. The β-decay of ^{14}C is an allowed ground-state to ground-state ($0^+ \rightarrow 1^+$) Gamow-Teller transition with an endpoint energy of $E_0 = 156$ keV and half life of 5730 yr. The ^{14}C spectrum in the CTF detector was studied in detail in [38].

The data are contaminated with the soft part of the spectra of beta and γ coming from the decay of ^{40}K[4]. A specific analysis has been performed, showing that the source is outside the inner vessel [37],[46]. The study of the optimal cut have been performed, with a cut radius varying from R=90 cm to R=110 cm, the final goal was to provide maximal surface background reduction with a minimal losses of the uniformly distributed over the detector's volume ^{14}C events. It was found that optimal ratio between the background reduction and detector's effective volume is achieved at R=100 cm. Using this cut the background reduction of the factor 5 in the energy region about 200 keV was achieved. At the same time only about 30% of the ^{14}C spectrum is lost in the region of interest.

[4] ^{40}K has two decay channels:
$^{40}K \rightarrow ^{40}Ca\,(\beta)$, 89.3%, $Q = 1.311\,MeV$,
$^{40}K \rightarrow ^{40}Ar\,(EC)$, 10.7%, $Q = 1.505\,MeV$,
the latter one is followed by the emission of 1.46 MeV γ.

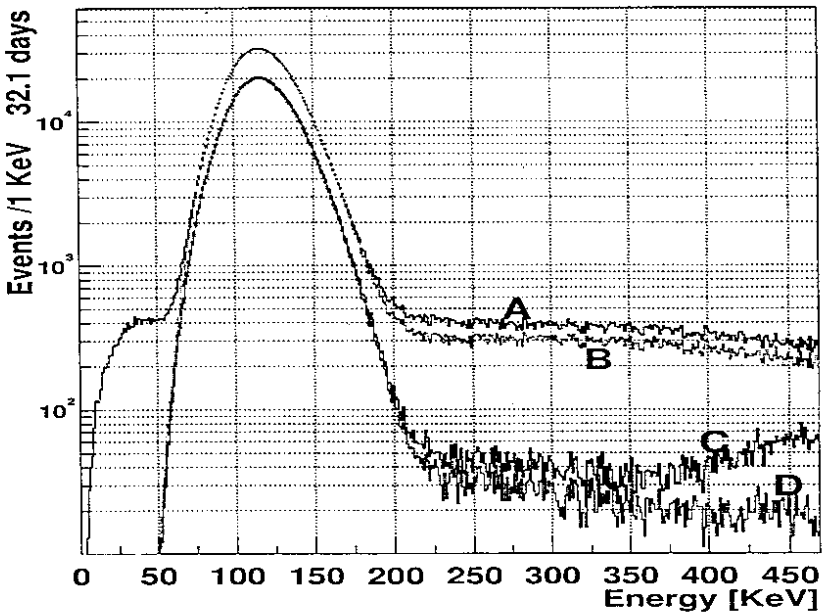

Figure 2: CTF-II background in the low energy region and the result of the sequential cuts applied in order to reduce background: A) raw data; B) muons cut; C) radial cut (with 100 cm radius); D)α/β discrimination.

Another possibility to reduce the background is to remove signals identified as muons by the muon veto system. The pulse shape analysis provides the possibility to distinguish between the signals caused by electrons and alpha- particles. In fig.2 all these cuts are shown. The residual spectrum in addition to the ^{14}C has the contribution of the other sources. This background is practically linear in the region 220-450 keV, and one can expect the same linear behaviour down to the lower limit used (138 keV). Monte Carlo simulations were performed to confirm the linear behaviour of this contribution the the total background. The simulation based on the measurements performed for the CTF-I detector indicate that the shape of the background underlying the ^{14}C $\beta-$spectrum has a small, constant slope for energies between 60 and 500 keV [38].

The part of the spectrum starting at 138 keV has been used in the analysis in order to avoid the spectrum distortions introduced by the threshold effect. The lower limit was estimated with Monte Carlo method taking into account the spatial distribution of the events, the electronics threshold (the electronics channel is fired if signal on the input overcomes discriminator threshold set at 0.2 p.e. level) and

the map of working PMTs. The simulation gives 45 p.e. lower limit (or 138 keV).

4 Neutrino-electron elastic scattering

4.1 Theory

As it was shown before, the study of the neutrino- electron scattering is the most sensitive test for the neutrino magnetic moment. In standard theory, scattering of a neutrino with a magnetic moment is determined both by weak interaction and by the one-photon exchange; the helicities of the initial and the final neutrino states are the same in the former case and different in the latter case. Therefore, the amplitudes of weak and magnetic scattering do not interfere, and the total cross section is the sum of the cross sections. For magnetic moment expected in the SM the contribution of the magnetic moment in the (ν, e)-scattering cross section is negligibly small.

The differential cross section of weak scattering of an electron neutrino by electron in the standard theory has the form:

$$\frac{d\sigma_{\mathrm{W}}}{dT_e}(T_e, E_\nu) = 4\sigma_0 \left[g_L^2 + g_R^2 \left(1 - \frac{T_e}{E_\nu}\right)^2 - g_L g_R \frac{T_e m_e}{2E_\nu^2} \right], \tag{6}$$

where $\sigma_0 = \frac{G_F^2 m_e}{2\pi} = 4.28 \times 10^{-45} \frac{cm^2}{MeV}$, the values of g_R and g_L depend only on the Weinberg angle $g_R = sin^2(\Theta_W)$, $g_L = \frac{1}{2} + sin^2(\Theta_W)$, and E_ν and T_e are the energies of the incident neutrino and the recoil electron. The (ν, e)-scattering cross section associated with the magnetic moment is:

$$\frac{d\sigma_{\mu_\nu}}{dT_e}(T_e, E_\nu) = \pi \cdot r_0^2 \cdot \mu_\nu^2 \left(\frac{1}{T_e} - \frac{1}{E_\nu}\right), \tag{7}$$

where μ_ν is neutrino magnetic moment measured in Bohr magnetons μ_B, and $r_0 = 2.818 \times 10^{-13}\ cm$ is the classical electron radius. The energy dependence of the cross sections of magnetic and weak scattering differ considerably; for $T_e \ll E_\nu$ their ratio is proportional to $\frac{1}{T_e}$, i.e., a reduction of the electron detection threshold should increase the sensitivity of the experiment to the magnetic moment. To get the expected energy spectrum of recoil electrons in detector it is necessary to average cross sections (6) and (7) over the neutrino spectrum $\phi_\nu(E)$:

$$\frac{dN}{dT_e}(T_e) = \int_{E_{\nu_{min}}(T_e)}^{E_{\nu_{max}}} \frac{d\sigma}{dT_e}(T_e, E_\nu)\phi_\nu(E_\nu)dE_\nu. \tag{8}$$

In this expression, $E_{\nu_{min}}(T_e) = \frac{T_e}{2}(1 + \sqrt{1 + \frac{2m_e}{T_e}})$ is the minimum energy of the neutrino at which a recoil electron with an energy T_e can be generated.

In the calculations we used SSM fluxes given by the standard solar model[47] and neutrino energy spectra from [48]. We assumed the independence of the magnetic moment on the neutrino flavour also. Signal shapes (8) were convolved with the detectors response function :

$$S(Q) = N_0 \int \frac{dN}{dT_e}(T_e(Q'))\frac{dT_e}{dQ} Res(Q, Q')dQ' \tag{9}$$

where $Res(Q, Q') = \frac{1}{\sqrt{2\pi}\sigma_Q} e^{-\frac{1}{2}(\frac{Q-Q'}{\sigma_Q})^2}$ is the detector response function, σ_Q is defined by (5).

4.2 Analysis

The data obtained during 32.1 days of the CTF-II were used. The CTF-II spectrum has been analyzed in the energy region 138-300 keV. The maximum likelihood method was used to find the possible additional part from the weak and electromagnetic scattering of the SSM solar neutrino in measured spectrum. The experimental spectrum was fitted with a sum of C-14 spectrum, additional linear background and spectrum of recoil electrons, due to pp- and ^7Be neutrino scattering by electron calculated in accordance to (6) and (7).

In order to avoid systematic errors, caused by the uncertainty of the linear part of the background, we were not fixing the parameters of the line describing this background, even its slope can be found from the Monte Carlo simulations. This is rather conservative approach.The only restriction applied was a negative slope of the linear background.

It was found that sensitivity of the detector to the weak interacting pp-neutrinos is about 23 times of the flux predicted SSM, i.e. $\phi(pp) \leq 23\phi_{SSM}(pp)$ at 90% c.l. The expected spectra for the SSM neutrino electromagnetic scattering are shown in fig.3 (pp-neutrino and ^7Be neutrinos). In assumption that neutrinos of all flavors have the equal magnetic moment the analysis of the likelihood function gives the upper limit of $\mu_\nu^{Sol} \leq 5.5 \times 10^{-10}\mu_B$ (90% c.l.). This value is the first one obtained for the low energy neutrino in direct experiment.

5 Radiative decay of neutrino

5.1 Theory

If neutrino would have mass, then the heavier one could decay to the lighter one $\nu_H \rightarrow \nu_L + \gamma$. A search for its decay provides the information about neutrino mass and mixing [49]-[52]. The probability of radioactive decay in SM is very low $\frac{1}{\tau} \approx \left(\frac{m_{\nu_H}}{30eV}\right)^5 10^{-29} y^{-1}$[53]. If neutrino transition moment μ_{HL}^{eff} has value close to expected for μ_ν in SM (2), then from (3) lifetime of neutrino is $\tau \sim 10^{29}$years. Diagram for radiative neutrino decay is identical to the diagram giving neutrino magnetic moment. So the reasons (the same as for the right boson) that lead to

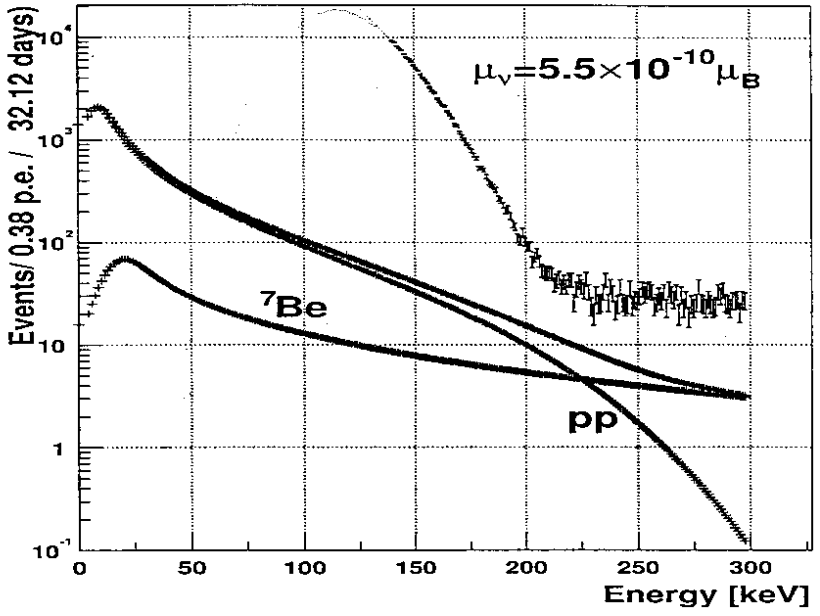

Figure 3: The experimental spectrum (upper plot with erroor bars) and the expected spectra for magnetic scattering of pp and ^7Be neutrinos calculated in accordance with () and ().

large magnetic moment also lead to the increase of the probability of radiative neutrino decay.

From now we will assume that the decaying neutrino ν_H is dominantly coupled to electron ($U_{eH} \approx 1$) and the vanishing neutrino mass in the neutrino in the final state ν_L (i.e. $m_{\nu_L} \ll m_{\nu_H}$). The expected laboratory gamma spectrum is defined by photon moment distribution in the center-of-mass system. For the common case one can write the photon angular distribution in the general form:

$$dN = \frac{1}{2}(1 + \alpha cos(\theta))dcos(\theta). \tag{10}$$

The anisotropy parameter α defines angular distribution of the photon relative to the spin of the decaying neutrino in the neutrino rest frame and relates to the space-time structure of the decay vertex. For the Majorana neutrino α is identically zero ($\alpha = 0$), but can take on any value $-1 \leq \alpha \leq 1$ for Dirac neutrino. In assumption of the total parity violation, the left (right)- handed Dirac neutrinos corresponds to the case $\alpha = -1(+1)$. The lab-frame energy of the decay gamma E_γ in the terms of the lab-frame energy of the neutrino E_ν and the center-of-mass angle θ is:

$$E_\gamma = \frac{E_\nu}{2}(1 + \frac{P_\nu}{E_\nu}cos(\theta)). \tag{11}$$

After the relativistic time dilation one obtains the energy gamma spectrum due to decay of the neutrino with energy E_ν:

$$\frac{dN}{dE_\gamma}(E_\gamma, E_\nu) = \frac{m_\nu}{\tau_{c.m.}}\frac{1}{E_\nu^2}(1 - \alpha + 2\alpha\frac{E_\gamma}{E_\nu}), \tag{12}$$

where $\tau_{c.m.}$ represents the center-of-mass neutrino lifetime. Taking into account the solar neutrino energy spectrum $\phi_\nu(E_\nu)$ one can write the expected gamma spectrum in the detector:

$$\frac{dN}{dE_\gamma}(E_\gamma) = \frac{VT}{c}\int_{E_\gamma}^{E_{\nu max}}\frac{dN}{dE_\gamma}(E_\gamma, E_\nu)\phi_\nu(E_\nu)dE_\nu. \tag{13}$$

where V is detector volume, T is time of measurement and c is the light speed in vacuum.

Experimentally the radiative decay of reactor antineutrino $\overline{\nu_e}$ have been studied in the works [55]-[59], the latter gives the best lifetime lower limit of $\tau_{c.m.}/m_\nu > 200\ s \cdot eV^{-1}, (\alpha = 0)$ (90% c.l.). The search for the ν_μ and $\overline{\nu_\mu}$ decay was performed in a high intensity beam of neutrinos from π^+ and μ^+ decays at rest. A lower bound on the lifetime of the muon (anti)neutrino $\tau_{c.m.}/m_{\nu_\mu} \geq 15.4s/eV, (\alpha = -1)$ was found in this experiment [60]. The astrophysical limits are more stronger and lies in the region $(10^9 - 10^{20}s/eV)$ [4],[61].

5.2 Analysis

The CTF can detect the gamma-quanta that appear in the neutrino radiative decay. The Monte Carlo method has been used in order to simulate the CTF response to the gammas. The neutrino decays in scintillator and in water were simulated separately and then summed taking into account the number of the candidate events. The response function was normalized to one neutrino decay in the scintillator volume.The program generates the gamma energy in accordance to the spectrum given by (13). Then the program generates random positions inside the inner vessel (or in the water layer of 30 cm) and follows the gamma- electron shower using the EGS-4 code[62]. As soon as an electron of energy E_e is to appear inside the scintillator, the corresponding charge is added to the running sum:

$$\Delta Q = E_e \cdot f(k_B, E_e) \cdot A \cdot f_R(r), \tag{14}$$

where $f_R(r)$ is a factor, taking into account the dependence of the registered charge on the distance from the detector's center. On the next step a random charge is generated in accordance to the normal distribution with a mean value of $Q = \sum \Delta Q$ and with variance σ_Q defined by formula (5). Finally, the radial reconstruction error was simulated in order to take into account the spatial cut applied.

The procedure of analysis was the same as in the case of search for neutrino magnetic moment. The analysis of likelihood function gives $\tau_{c.m.}/m_\nu > 4.2 \cdot 10^3\ s \cdot eV^{-1}$ ($\alpha = 0$), $\tau_{c.m.}/m_\nu > 9.7 \cdot 10^3\ s \cdot eV^{-1}$ ($\alpha = 1$) and $\tau_{c.m.}/m_\nu > 1.5 \cdot 10^3\ s \cdot eV^{-1}$ ($\alpha = -1$). The results of fitting for $\alpha = 0$ are shown on fig.4.

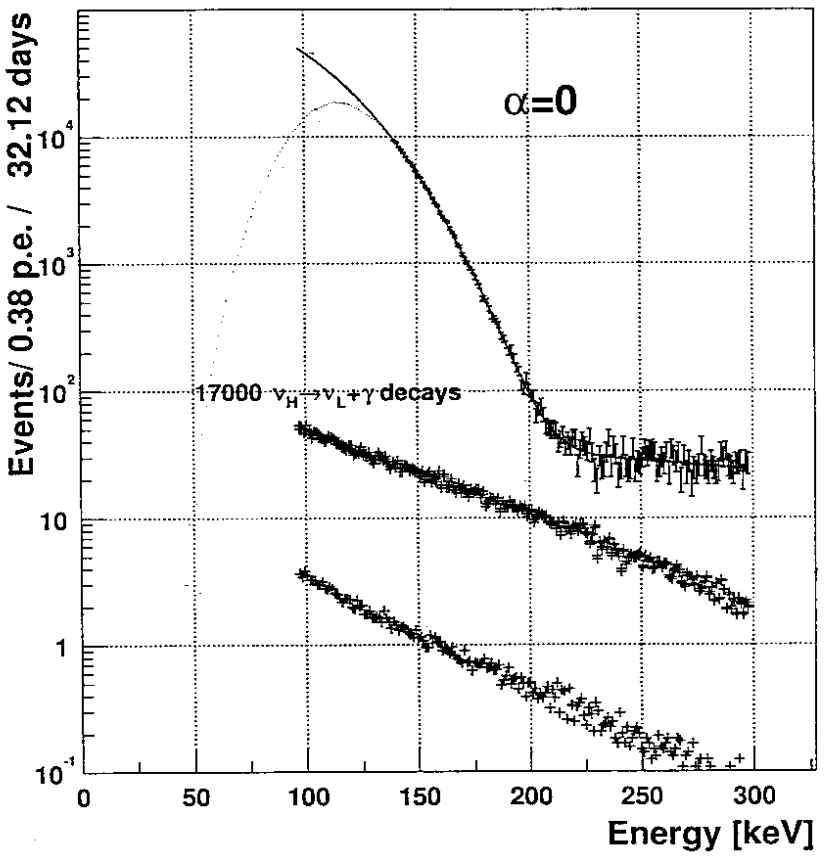

Figure 4: The results of fitting for $\alpha = 0$. The experimental spectrum (upper plot with erroor bars) and the results of the Monte Carlo simulation of 17000 $\nu_H \to \nu_L + \gamma$ decays in the scintillator are shown.

Using (3) one can compare the bound obtained for magnetic moment μ_ν and the bound for radiative lifetime of neutrino $\tau_{c.m.}/m_\nu$. For $m_{\nu_H} \approx \delta m \approx 1eV$, from lower limit on the lifetime of radiative neutrino decay $\tau_{c.m.}/m_\nu > 1.5 \cdot 10^3\ s \cdot eV^{-1}$

one expect that $\mu_{HL}^{eff} \leq 1.2 \cdot 10^{-2} \mu_B$. From the other side, in assumption that $\mu_\nu \approx \mu_{HL}$, from upper limit $\mu_\nu \leq 5.5 \cdot 10^{-10}\ \mu_B$ one obtaines that lifetime has to be $\tau_{c.m.}/m_\nu \geq 7 \cdot 10^{17}\ s \cdot eV^{-1}$.

6 Conclusions

The new upper limit on the magnetic moment of pp- and ^7Be neutrino has been established $\mu_\nu \leq 5.5 \times 10^{-10}\ \mu_B$. This value is only 3 times lower then obtained for reactor's neutrino and ^8B- solar neutrino. The new lower limit on the mean lifetime neutrino relative radiative decay is obtained $\tau_{c.m.}(\nu_H \to \nu_L + \gamma)/m_\nu \geq 1.5 \cdot 10^3\ s \cdot eV^{-1}$. It is more then one order of magnitude more than obtained in previous direct laboratory experiments. The CTF data can be used in the search of neutrino charge radius $< r^2 >$ and $\nu_H \to \nu_L + e^+ + e^-$ decay as well.

References

[1] Kayser B., PRD26 (1982) 1662

[2] Marinelli M., Morpurgo G., PLB137 (1984) 439

[3] Baumann J., et al., PRD37 (1988) 3107

[4] Groom D.E. et al (Particle Data Group), Eur. Phys. Jour. C15 (2000) 1

[5] Raffelt G.G., Phys.Rep., 320 (1999) 319

[6] Marciano W.J, Sirlin A., PRD22 (1980) 2695

[7] Vogel P., Engel J., PRD 39 (1989) 3378

[8] Allen R.C., et al., PRD47 (1993)113

[9] Ahrens L.A. et al PRD41 (1990) 3297

[10] Vilain P., et al., PL B345 (1995) 115

[11] Lobashev V.M. et al. Nucl.Phys. Proc.Suppl. 77B (1999) 327.

[12] Beg M.A., Marciano W.J., Ruderman M., PRD17 (1978) 1395

[13] Cowan C.L., Reines F., Harrison F.B., Phys.Rev., 96 (1954) 1294

[14] Cowan C.L., Reines F., Phys.Rev., 107 (1957) 528

[15] Bazilevskaya G.A., Stojkov Ju.I., Charahchay T.N., JETF Lett., 35 (1982) 273

[16] Gavrin B.N., Kopusov Ju.S., Makeev N.T., JETF Lett., 35 (1982) 491

[17] Bahcall J.N., Neutrino Astrophysics, Cambridge Univ.Press, Cambridge, 1989

[18] Voloshin M.B., Vysotskii M.I., Yad.Fiz., 44 (1986) 845

[19] Okun' L.B. Yad.Fiz., 44 (1986) 847

[20] Voloshin M.B., Vusotskii M.I., Okun' L.B., Yad.Fiz. 44 (1986) 677

[21] Walter G., Phys.Rev.Lett., 79 (1997) 4522

[22] Sturrock P.A., Walther G., Wheatland M.S., Astrophys.J. 507 (1998) 978

[23] Pulido J., Phys. Rep. 211 (1992) 211, hep-ph/0106201, hep-ph/0101116

[24] Akhmedov E.Kh. Phys.Lett., B213 (1988) 64, B348 (1995) 124

[25] Pulido J., Akhmedov E.Kh., Astropat.Phys. 13 (2000) 227

[26] Akhmedov E.Kh., Pulido J., Phys.Lett., B485 (2000) 178

[27] Derbin A.V., Yad.Fiz. 57 (1994) 236, Phys.At.Nucl. 57 (1994) 222

[28] LSND collaboration, hep-ex/0101039

[29] DONUT collaboration, hep-ex/0102026

[30] Raffelt G.G., Phys.Rep., 320 (1999) 319

[31] Pulido J., Mourao A.M., Phys.Rev. D57 (1998) 1794

[32] J.F.Beacom, P.Vogel PRL 83 (1999) 5222

[33] Voloshin M.I., Stefanov M.A., Yad.Fiz., 53 (1991) 1632

[34] Leure M., Marcus N., Phys.Lett. H237 (1990) 81

[35] Borexino Collaboration, G.Alimonti et al., Astrop.Journal 2001

[36] Borexino Collaboration, G.Alimonti et al., Nucl.Instr.Meth. A406 (1998) 411

[37] Resconi E., "Measurements with the Upgraded Counting Test Facility (CTF-2) of the Solar Neutrino Experiment Borexino", Doctorate Thesis, Universita' degli Studi di Genova, 2001

[38] Borexino Collaboration, Alimonti G., et al., Phys.Lett. B422 (1998) 349

[39] Borexino Collaboration, Alimonti G.,et al., Astroparticle Phys. 8 (1998) 141

[40] Borexino Collaboration, Alimonti G.,et al., Nucl.Instr.Meth. A440 (2000) 360

[41] Ranucci G., et al., Nucl.Instr.Meth. A333 (1993) 553

[42] Birks J.B., Proc.Phys.Soc. A64 (1951) 874.

[43] Bonetti S., Donghi O., Salvo C., Testera G., "Ionization quenching: effects on e^- and γ detection in Borexino and in CTF". Borexino internal report 98/10/15, 1998.

[44] Smirnov O., Resolutions of a large volume liquid scintillator detector. LNGS preprint INFN TC/00/17 (2000).

[45] Borexino collaboration. Search for electron decay mode $e \rightarrow \gamma + \nu$ with prototype of Borexino detector. Accepted by Nucl.Phys.B

[46] Cadonati L., Borexino internal report, 00/08/27 (2000).

[47] J. N. Bahcall, H. Pinsonneault, and Sarbani Basu, astro-ph/0010346

[48] J.N. Bahcall. Phys. Rev. C. 56 3391(1997).

[49] Petcov S.T., Yad.Fiz., 25 (1977) 641

[50] Sato E., Kobayashi M., Prog.Theor.Phys., 58 (1977) 1775

[51] De Rujula A., Glashow S.L., Phys.Rev.Lett., 45 (1980) 942

[52] Pal P.B., Wolfenstein L., Phys.Rev. D25 (1982) 766

[53] Boem F., Vogel P., Physics of massive neutrinos, ed. MIR, (1990) 113

[54] Shrock R..E. Nucl.Phys.,B296 (1982) 359

[55] Reines F., et al., Phys.Rev.Lett., 32 (1974) 180

[56] Vogel P., Phys.Rev., D30 (1984) 1505

[57] Zacek G. et al, Phys.Rev. D34 (1986) 2621

[58] Oberauer L., Von Feilitzsch F., Mossbauer R.L., Phys.Lett., B198 (1987) 113

[59] Derbin A.V. et al., JETP Lett., 57 (1993) 755

[60] Krakauer D.A., et al., PRD 44 (1991) 44

[61] Oberauer L., et al Astrparticle Phys., 1 (1993) 377

[62] Walter R. Nelson, Hideo Hirayama, David W. O. Rogers. The EGS4 code system. SLAC-265, 1985.

Received on February 22, 2002.

SUBJECT CATEGORIES OF THE JINR PUBLICATIONS

Index	Subject
1.	High energy experimental physics
2.	High energy theoretical physics
3.	Low energy experimental physics
4.	Low energy theoretical physics
5.	Mathematics
6.	Nuclear spectroscopy and radiochemistry
7.	Heavy ion physics
8.	Cryogenics
9.	Accelerators
10.	Automatization of data processing
11.	Computing mathematics and technique
12.	Chemistry
13.	Experimental techniques and methods
14.	Solid state physics. Liquids
15.	Experimental physics of nuclear reactions at low energies
16.	Health physics. Shieldings
17.	Theory of condensed matter
18.	Applied researches
19.	Biophysics

Бек Х. О. и др.
E1-2002-29

Изучение электромагнитных свойств нейтрино
на прототипе детектора «Борексино»

Результаты измерений на прототипе детектора «Борексино» позволили установить верхние пределы величин магнитного момента μ_ν и времени жизни нейтрино относительно распада $\nu_H \to \nu_L + \gamma$. Новый предел μ_ν для *pp*- и ^{7}Be-солнечных нейтрино составляет $5{,}5 \cdot 10^{-10}\ \mu_B$, а время жизни — $\tau_{c.m.}(\nu_H \to \nu_L + \gamma)/m_\nu \geq 1{,}5 \cdot 10^3$ с·эВ$^{-1}$. Последний результат на порядок лучше предела, полученного ранее в экспериментах с реакторными нейтрино.

Работа выполнена в Лаборатории физики частиц ОИЯИ.

Препринт Объединенного института ядерных исследований. Дубна, 2002

Back H. O. et al.
E1-2002-29

Study of the Neutrino Electromagnetic Properties
with Prototype of Borexino Detector

Results of background measurements with the prototype of the Borexino detector have been used to obtain upper bound on neutrino magnetic moment μ_ν and lifetime of radiative neutrino decay $\nu_H \to \nu_L + \gamma$. The new upper limit for μ_ν of *pp* and ^{7}Be neutrino is $5.5 \cdot 10^{-10}\ \mu_B$ and lifetime $\tau_{c.m.}(\nu_H \to \nu_L + \gamma)/m_\nu \geq 1.5 \cdot 10^3$ s·eV^{-1}. The latter result is an order of magnitude more restrictive than obtained in previous laboratory experiments.

The investigation has been performed at the Laboratory of Particle Physics, JINR.

Preprint of the Joint Institute for Nuclear Research. Dubna, 2002

Макет *Т. Е. Попеко*

ЛР № 020579 от 23.06.97.
Подписано в печать 11.04.2002.
Формат 60 × 90/16. Бумага офсетная. Печать офсетная.
Усл. печ. л. 1,18. Уч.-изд. л. 1,9. Тираж 555 экз. Заказ № 53227.

Издательский отдел Объединенного института ядерных исследований
141980, г. Дубна, Московская обл., ул. Жолио-Кюри, 6.